 CMES, vol.18, no.2, pp.121-144, 2007

Buckling and Free Vibrations of Sandwich General shells of Revolution with Composite facings and Viscoelastic core under Thermal Environment using Semi-analytical Method

Sharnappa[1], N. Ganesan[2] and Raju Sethuraman[3]

Abstract: This article presents the study on buckling and free vibration behavior of sandwich general shells of revolution under thermal environment using Wilkins theory. The temperature assumes to be uniform over the shell structure. The numerical analysis is based on the semi-analytical finite element method applicable to thick shells. The analysis is carried out for different geometry such as truncated conical and hemispherical shells with various facing and core materials under clamped-clamped boundary condition. The parametric study is carried out for different core to facing (t_c/t_f) thickness ratio by considering the temperature dependent and independent material properties of the viscoelastic cores.

Keyword: Vibration, Complex modulus, Thermal environment, Buckling analysis.

1 Introduction

The sandwich structures with constrained viscoelastic core are being used in various engineering application, particularly for vibration control of wide range of frequencies. The dissipation of energy in core material reduces the vibration of the structures. The sandwich layered shell (*viz.* cylindrical, conical and spherical) constructions are widely used in aircraft, missile, space vehicle structures and nuclear power plants. In recent years, few studies have been carried out on free vibrations of sandwich shells with viscoelastic core under thermal environment, and damping evaluation of the layered shells.

Recently, the studies on buckling and free vibration of shells under thermal environment are gaining higher research importance. Pradeep, Ganesan and Padmanabhan (2006) are investigated the buckling and vibration of a viscoelastic sandwich cylindrical shell under thermal environment. Singh and Subramaniam (2003) presented the vibration of thick circular disks and shells of revolution for free axisymmetric and asymmetric vibrations problems by using three-dimensional theory of elasticity. Pei and Issam (1992) presented an iterative numerical method for the analysis of axisymmetric, isotropic general shells with varying wall rigidity. Shell elements of special geometric shapes, e.g., cylindrical, spherical, and conical shells, are also considered. They have used the one-dimensional finite difference points to discretise the shell elements into strips along the meridian. Tan (1998) investigated the free vibration analysis of shells of revolution using first order shear deformation theory as well as the classical thin shell theory.

Arthur and Jae (1999, 2004, 2006) presented the three dimensional analysis for determining the free vibration frequencies and mode shapes of hollow shells of revolution with variable thickness. They have extended the study to complete (not truncated) conical shells of revolution and also to thick conical shell of revolution with the bottom edge normal to the mid-surface in circular cylindrical co-ordinate system. Bradell, Langley, Dunsdon and Aglietti (1998-99) investigated the study on vibration analysis of a general three-layer conical sandwich panel based on

[1] Research Scholar, Department of Mechanical Engineering, Indian Institute of Technology Madras, Chennai, India 600 036.

[2] Professor, Corresponding author, Department of Mechanical Engineering, Indian Institute of Technology Madras, Chennai, India 600 036. nganesan@iitm.ac.in

[3] Professor, Department of Mechanical Engineering, Indian Institute of Technology Madras, Chennai, India 600 036.

the $h-p$ version of the finite element method. They also studied the free vibration behaviour of thin isotropic conical panels in conjunction with Love's thin shell equations. Buchanan and Wong (2001) studied the vibration of truncated thick hollow cones employing finite element method in conical co-ordinate system.

Yuh and Shyh (2000) are derived the general differential equations of motion for a three-layer sandwich structure with viscoelastic core by using Hamilton's and Donnell-Mushtari-Vlasov principles. The proposed theory can be used for analyzing the different geometrical structures such as cylindrical, conical, spherical shells and plates. Ramasamy and Ganesan (1999) presented the vibration and damping analysis of fluid filled orthotropic cylindrical shells with constrained viscoelastic damping by using Wilkin's theory. Khatri (1996) investigated the antisymmetric vibration of multilayered conical shells with constrained viscoelastic layers. The study has been extended along with Asnani (1995-96) to the vibration and damping analysis based on individual layer deformation for axisymmetric vibrations of laminated composite conical shells. Sivadas and Ganesan (1992, 1995) analyzed the vibration behaviour of pre stressed thick circular conical isotropic and composite shells, by using semi-analytical isoparametric finite element method. They are considered three nodes per element with five degrees of freedom per node. Liyong (1993) also presented the free vibration of composite laminated conical shells.

Wilkins, Bert and Egle (1970) have studied the free vibration analysis of orthotropic conical shell with honeycomb core sandwich structures. The effect of shear deformation is accounted for the facings. Ravikiran and Ganesan (2005) investigated a theoretical analysis of linear thermo elastic buckling of composite hemispherical shells with a cut out at the apex. They have used the semi-analytical finite element method applicable to moderately thick shells. Okazaki, Urata and Tatemichi (1990) investigated damping properties of three layered shallow spherical shells with a constrained viscoelastic layer. Natural frequencies and loss factors of shallow spherical shells are evaluated for axially and nonaxially symmetric modes.

Gautham and Ganesan (1994) presented the free vibration analysis of thick spherical shells. They developed the thick shell finite element for the analysis of general shells of revolution and used for the spherical shells. Chen and Ding (2001) are carried out three-dimensional analysis for the free vibrations of a multi layered spherically isotropic hollow sphere using a state space method based on Taylor's expansion theorem. De Souza and Croll (1980-81) investigated the free vibrations of isotropic spherical shells using a variational development of the equations of motion based upon classical shell theory and extended to study the composite spherical shell. Recently Jones (2005) investigated the thermal buckling of uniformly heated fiber reinforced composite plates. The analysis is restricted to linear elastic stress-strain behavior and constant orthotropic lamina material properties at a specific temperature. The parametric study is considered for various composite materials in different boundary conditions.

Recently some of the buckling study has been carried out on sandwich structure such as, Pahr and Rammerstorfer (2006) presented the buckling of honeycomb sandwiches structures using finite element method, the influence of core thickness, core material and facings thickness on buckling load is investigated. Li, Xiang and Xue (2005) presented the buckling analysis of honeycomb sandwich composite shells with cutouts under axial compression, using the Wilson's incompatible solid Finite Element. Baiz and Aliabadi (2006) studied the linear buckling analysis of shear deformable shallow shells by the boundary element method. Jihan, Yong and Sung (2004) are analyzed the asymptotic postbuackling of composite sandwich structures using the assumed strain solid shell element formulation. Ching and Chen (2006) investigated the thermomechanical analysis of functionally graded composites structure using Meshless Local Pstrov-Galerkin method. Chih, Jyh and Jyh (2005) investigated an asymptotic theory of doubly curved laminated piezoelectric shells is developed on the basis of three-dimensional (3D) linear piezoelectricity. Shiah,

Lin and Tan (2006) presented the stress analysis of thin-layered anisotropic bodies using boundary element method and also validated with finite element method.

The buckling and free vibration analysis of sandwich general shells of revolution under thermal environment by considering the pre-stresses is not found in the literature. The present study investigates the buckling temperature, frequency and loss factor of sandwich truncated conical shell and hemispherical shell with composite facings and viscoelastic core material. There are three types of composite facing materials and two types viscoelastic materials such as EC2216 and DYAD606 by considering the temperature dependent and independent properties core are used in the present study, which are reported by Jones (2005) and Nashif, Jones and Henderson (1985). The detail study has been carried out for sandwich truncated conical shell, and some of the typical results of hemispherical shell with cut out at a apex also discussed.

2 Finite element formulation

In the present study, the FORTRAN code is developed for viscoelastic general shells of revolution under thermal environment. Since the structure is axisymmetric, semi analytical finite element method is used. Displacement distributions are expressed in terms of Fourier series expansion in the circumferential direction. The displacement assumption in the thickness direction is based on Wilkins theory. Figure 1 shows the schematic diagram of sandwich general shells of revolution. The displacement field used in the analysis is proposed by Wilkins, Bert and Egle (1970), the displacements u, v, w are along s, θ and z coordinate directions respectively. The above displacements are defined in terms of middle surface displacements (u_0, v_0, w_0) and the angles of rotation normal to the middle surface in the meridian (s) and circumferential (θ) directions, for the facings and core angles are denoted by ϕ_s, ϕ_θ and ψ_s, ψ_θ respectively. Assumptions made by Wilkins, Bert and Egle (1970) and Ramasamy and Ganesan (1999) are applicable in the present study in addition to that, there is no slip between the core and facings, the interface between the core and facings are firmly bounded.

The displacement relations for the core is given by

$$\begin{aligned} u^c &= u_0 + z\,\psi_s \\ v^c &= v_0 + z\psi_\theta \\ w^c &= w_0 \end{aligned} \tag{1}$$

The displacement relations for the outer and inner facings respectively are given by

$$\begin{aligned} u^o, u^i &= u_0 \pm h\psi_s + (z \mp h)\phi_s \\ v^o, v^i &= v_0 \pm h\psi_\theta + (z \mp h)\phi_\theta \\ w^o, w^i &= w_0 \end{aligned} \tag{2}$$

Here z denotes the distance from the middle surface of the shell and h is half the core thickness.

The strain displacement relations for the core, outer and inner facings are same as referred by Ramasamy and Ganesan (1999). Since the structure is axisymmetric, semi analytical finite element method is used in meridional direction and Fourier expansion is used in the circumferential direction. Three nodded isoparametric element with seven degrees of freedom per node is used for the structure. There are 20 elements used along the meridional direction. The displacement parameters associated with the elements are

$$\begin{aligned} &\{\delta^e\} = \\ &\quad \{u_{0,1}\, v_{0,1}\, w_{0,1}\, \psi_{s,1}\, \psi_{\theta,1}\, \phi_{s,1}\, \phi_{\theta,1} \cdots\cdots \phi_{s,3}\, \phi_{\theta,3}\} \end{aligned} \tag{3}$$

Where, the subscripts 1, 2 and 3 denotes the node number.

The assumed displacement distributions are as follows. Fourier expansion is used in the circumferential direction.

$$u_0 = \sum_{i=1}^{i=3} N_i u_{0,i} \cos n\theta \qquad \psi_\theta = \sum_{i=1}^{3} N_i \psi_{\theta,i} \sin n\theta$$

$$v_0 = \sum_{i=1}^{3} N_i v_{0,i} \sin n\theta \qquad \phi_s = \sum_{i=1}^{3} N_i \phi_{s,i} \cos n\theta$$

$$w_0 = \sum_{i=1}^{3} N_i w_{0,i} \cos n\theta \qquad \phi_\theta = \sum_{i=1}^{3} N_i \phi_{\theta,i} \sin n\theta$$

$$\psi_s = \sum_{i=1}^{3} N_i \psi_{s,i} \cos n\theta$$

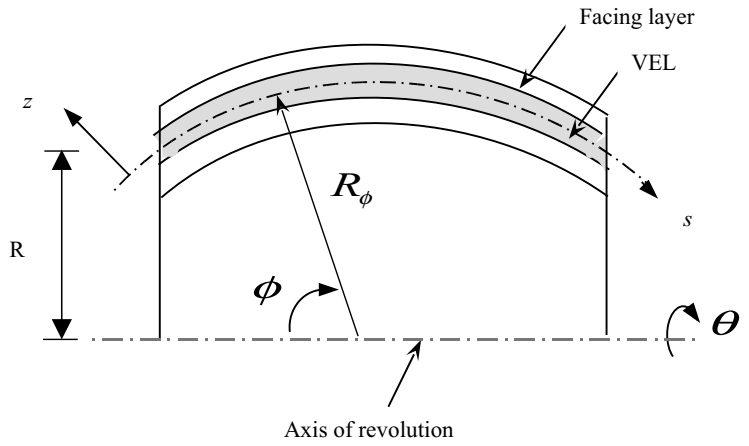

Figure 1: Schematic diagram of general shell with constrained viscoelastic core

(4)

where , N_i is the shape functions given by

$$N_1 = (\xi^2 - \xi)/2 \quad N_2 = 1 - \xi^2 \quad N_3 = (\xi^2 + \xi)/2 \tag{5}$$

Here $\xi = s/l$ is the isoparametric axial coordinate (l is the length of the element), n is the circumferential mode number. By using equations (1), (2), (4) and (5) the displacement vector can be written in matrix form as

$$\{u_1\} = [N]\{\delta^e\} \tag{6}$$

Where $\{u_1\}^T = \{u\, v\, w\}$, $[N]$ is shape function matrix and $\{\delta^e\}$ is the vector of nodal displacements. Substituting (4) in strain-displacement relation the array of strains $\{\varepsilon\}$ can be written as

$$\{\varepsilon\}^T = \{\varepsilon_{ss}\, \varepsilon_{\theta\theta}\, \gamma_{s\theta}\, \gamma_{\theta z}\, \gamma_{sz}\} = [B_\theta]\{\delta_n^e\} \tag{7}$$

where $[B_\theta] = [B](\cos\theta \text{ or } \sin\theta)$ and here $[B]$ is the strain displacement matrix. $\{\delta_n^e\}$ is the vector of nodal displacements for the n^{th} harmonic.

The stress strain relations, accounting the thermal effects in the shell coordinate for a j^{th} layer can be expressed as

$$\begin{Bmatrix} \sigma_{ss} \\ \sigma_{\theta\theta} \\ \tau_{s\theta} \\ \tau_{sz} \\ \tau_{\theta z} \end{Bmatrix}_j = \begin{bmatrix} \overline{Q}_{11} & \overline{Q}_{12} & \overline{Q}_{16} & 0 & 0 \\ \overline{Q}_{12} & \overline{Q}_{22} & \overline{Q}_{26} & 0 & 0 \\ \overline{Q}_{16} & \overline{Q}_{26} & \overline{Q}_{66} & 0 & 0 \\ 0 & 0 & 0 & \overline{Q}_{44} & 0 \\ 0 & 0 & 0 & 0 & \overline{Q}_{55} \end{bmatrix}_j \cdot \left(\begin{Bmatrix} \varepsilon_{ss} \\ \varepsilon_{\theta\theta} \\ \gamma_{s\theta} \\ \gamma_{sz} \\ \gamma_{\theta z} \end{Bmatrix} - \begin{Bmatrix} \alpha_{ss}\Delta T \\ \alpha_{\theta\theta}\Delta T \\ 0 \\ 0 \\ 0 \end{Bmatrix} \right)_j \tag{8}$$

Where

$$\overline{Q}_{11} = Q_{11}C^4 + 2(Q_{12} + 2Q_{66})S^2C^2 + Q_{22}S^4$$

$$\overline{Q}_{12} = (Q_{11} + Q_{22} - 4Q_{66})S^2C^2 + Q_{12}(S^4 + C^4)$$

$$\overline{Q}_{22} = Q_{11}S^4 + 2(Q_{12} + 2Q_{66})S^2C^2 + Q_{22}C^4$$

$$\overline{Q}_{16} = (Q_{11} - Q_{12} - 2Q_{66})SC^3 + (Q_{12} - Q_{22} + 2Q_{66})S^3C$$

$$\overline{Q}_{26} = (Q_{11} - Q_{12} - 2Q_{66})S^3C + (Q_{12} - Q_{22} + 2Q_{66})SC^3$$

$$\overline{Q}_{66} = (Q_{11} + Q_{22} - 2Q_{12} - 2Q_{66})S^2C^2 + Q_{66}(S^4 + C^4)$$

$$\overline{Q}_{44} = Q_{44}C^2 + Q_{55}S^2$$

$\overline{Q}_{55} = Q_{44}S^2 + Q_{55}C^2$

where $C = \cos\theta$ and $S = \sin\theta$; θ is Fiber angle

α_{ss} and $\alpha_{\theta\theta}$ are co-efficient of thermal expansion in 's' direction (meridional direction) and 'θ' direction (Circumferential direction) respectively. $\Delta T = (T - T_0)$ =Change in Temperature, here T is actual system temperature and T_0 is reference or atmospheric temperature. $[Q]$ is the elasticity matrix in the material co-ordinates, the elements of the $[Q]$ are

$$\begin{aligned} &Q_{11} = E_L/(1-\upsilon_{LT}\upsilon_{TL}), \\ &Q_{22} = E_T/(1-\upsilon_{LT}\upsilon_{TL}), \\ &Q_{12} = \upsilon_{TL}Q_{11}, \qquad && Q_{44} = G_{TZ}; \\ &Q_{55} = G_{TL}; && Q_{66} = G_{LT}, \end{aligned}$$

For Viscoelastic core $G^* = G_R(1+i\eta) = G_R + G_I$. Where E_L is Young's modulus in longitudinal direction, E_T is Young's modulus in transverse direction, G* is Complex shear modulus, G_R is Storage modulus, η is loss factor and G_I Loss modulus given by Nashif, Jones and Henderson (1985) shown in the Figure 2, ν_{LT} and ν_{TL} are Poisson's ratio. In equation (8) subscript $j = o, c, i$ denotes the outer facing, core and inner facings respectively. The equation (8) can be written in simplified version as

$$\{\sigma\} = [D^j]\left(\{\varepsilon^j\} - \{\varepsilon^{jth}\}\right) \tag{9}$$

where $[D^j]$ is material properties matrix $\{\varepsilon^j\}$, $\{\varepsilon^{jth}\}$ are the arrays of generalized mechanical and thermal strains in the j^{th} layer.

Under thermal environment the total potential U_1 for the sandwich shell element can be written as

$$U_1 = \frac{1}{2}\sum_{j=o,c,i}\iiint_v \{\varepsilon^j\}^T[D^j]\left(\{\varepsilon^j\} - \{\varepsilon^{jth}\}\right) \cdot r^j d\theta ds dz \tag{10}$$

Where super script $j = o$, c, i denotes the outer facing, core and inner facings respectively, r^j is the mean radius of the j^{th} layer. Using equation (7) in equation (10) and carrying out explicit integration in the θ direction (there by minimizing U_1 with respect to $\{\delta^e\}$) leads to the following equation.

$$C\left(\int [B]^T[D][B]\{\delta^e\} r ds - \int [B]^T[D]\{\varepsilon^{th}\} r ds\right) = 0 \tag{11}$$

After decoupling each harmonic n, the following equation for the n^{th} harmonic can be arrived at

$$[K_n^e]\{\delta_n^e\} - \{F_n^{the}\} = 0 \tag{12}$$

Where $[K_n^e]$ is element stiffness matrix given by

$$[K_n^e] = C\int [B_n]^T[D][B_n] r ds \tag{13}$$

$\left\{F_n^{the}\right\}$ is a element thermal load vector given by

$$\{F_n^{the}\} = C\int [B_n]^T[D]\{\varepsilon^{th}\} r ds \text{ for } n^{th} \text{ harmonic} \tag{14}$$

In the above equations $C = 2\pi$ and π for $n = 0$ and $n > 0$ respectively. The superscript e over the matrix indicates that it is an elemental matrix and subscript n indicates the harmonic number. Since the properties of the core and also some of the composite facing materials are complex, so the stiffness matrix is a complex. It can be written as

$$[K_n^e] = [K_{nR}^e] + i[K_{nI}^e] \tag{15}$$

$[K_{nR}^e]$ is the real part and $[K_{nI}^e]$ is the imaginary part.

The expression for the mass matrix can be obtained from the expression of kinetic energy as follows

$$KE = \frac{1}{2}\int_v \{\dot{u}_1\}^T[\rho]\{\dot{u}_1\} r d\theta ds dz \tag{16}$$

where $\{u_1\}^T = \{u\, v\, w\}$ and the dot over vector indicates variable derivative with respect to time. ρ is density of the structure. Making use of equation (4) in the expression for $\{\dot{u}_1\}$ and carrying out explicit integration in the θ direction, equation (16) can be written as

$$KE = \frac{C}{2}\{\dot{\delta}^e\}^T \iint [N]^T[\rho][N]\{\dot{\delta}^e\} r ds dz \tag{17}$$

The element mass matrix for the n^{th} harmonic can be written as

$$[M_n^e] = C\int [N]^T[\rho][N] r ds \tag{18}$$

2.1 Geometric Stiffness Matrix

The present study deals with linear bifurcation buckling analysis of sandwich shells. The geometric stiffness matrix can be obtained from the expression of work done by the initial stresses considering nonlinear strains.

The strain energy due to nonlinear strains and initial stresses is given by

$$U_g = \frac{1}{2}\int_v \left(\left((\varepsilon_{ss})_g \right)^2 \sigma_{ss}^{+} 2 (\gamma_{s\theta})_g \tau_{s\theta}^{+} \left((\varepsilon_{\theta\theta})_g \right)^2 \sigma_{\theta\theta} \right) \cdot r\, ds\, d\theta\, dz \quad (19)$$

where

$$(\gamma_{s\theta})_g = (\varepsilon_{ss})_g (\varepsilon_{\theta\theta})_g$$

The non-linear strains are given by

$$\begin{aligned} (\varepsilon_{ss})_g &= k_1 \left(\frac{\partial w}{\partial s} - \frac{u}{R_\phi} \right); \\ (\varepsilon_{\theta\theta})_g &= k_2 \left(\frac{1}{r}\frac{\partial w}{\partial \theta} - \frac{v}{r}\sin\phi \right) \end{aligned} \quad (20)$$

where

$$k_1 = \frac{1}{\left(1 + \frac{z}{R_\phi}\right)} \quad \text{and} \quad k_2 = \frac{1}{\left(1 + \frac{z}{R_\theta}\right)}$$

The equation (19) can be written in matrix form as follows

$$U_g = \frac{1}{2}\sum_{j=o,i}\int_v \begin{Bmatrix} (\varepsilon_{ss})_g^j \\ (\varepsilon_{\theta\theta})_g^j \end{Bmatrix}^T \begin{bmatrix} \sigma_{ss}^j & \tau_{s\theta}^j \\ \tau_{s\theta}^j & \sigma_{\theta\theta}^j \end{bmatrix} \begin{Bmatrix} (\varepsilon_{ss})_g^j \\ (\varepsilon_{\theta\theta})_g^j \end{Bmatrix} dv \quad (21)$$

Where the super script $j = o, i$ indicates the outer and inner stiff (facing) layers.

The equation (21) can be re written in simplified manner as follows

$$U_g = \frac{1}{2}\sum_{j=o,i}\int_v \left(\{B_g\}^j \right)^T [\sigma_g]^j \{B_g\}^j r\, ds\, d\theta\, dz \quad (22)$$

Carrying out explicit integration in θ direction, equation (22) can be written as

$$U_2 = \frac{C}{2}\{\delta^e\}^T \iint [B_g]^T [\sigma_0][B_g]\{\delta^e\} r ds dz \quad (23)$$

After decoupling each harmonic n, the following expression can be expressed for evaluating the geometric stiffness matrix at n^{th} harmonics as.

$$[K_{gn}^e] = C \iint [B_{gn}]^T [\sigma_0] B_{gn}] r ds\, dz \quad (24)$$

The element matrices are assembled to get the global stiffness $[K]$ (which is complex), mass $[M]$ matrices and geometric stiffness matrix $[K_g]$ for each circumferential mode.

2.2 Buckling analysis

The buckling temperatures of a sandwich shell can be found by solving the following eigenvalue problem

$$[K_{nR}] + \lambda_n [K_{gn}] = 0 \quad (25)$$

Where $[K_{nR}]$ and $[K_{gn}]$ are global real part of the stiffness matrix and global geometric stiffness matrix obtained after assembly (refer to equations (15) and (24)). $[K_{gn}]$, is formulated at a reference temperature T_{ref} and the eigenvalue problem of equation (25) is solved. The approximate critical buckling temperature for the n^{th} circumferential mode and m^{th} axial mode of the shell is given by $T_b = (\lambda_n)_m T_{ref}$ where $(\lambda_n)_m$ is the buckling parameter for n^{th} circumferential mode and m^{th} axial mode. In general viscoelastic material properties are strongly temperature dependant, but the properties of facing materials assumed to be constant in the operating range considered in this paper (Typically less than 300°C).

2.3 Evaluation of Frequency and Loss factor

The following eigen value problem has to be solved to get the natural frequencies for each harmonics under thermal environment.

$$[K_{nR} + K_{gn}] - \omega^2 [M_n] = 0 \quad (26)$$

Where ω is the natural frequency and $[K_{gn}]$ is the geometric stiffness matrix for n^{th} harmonic.

The viscoelastic and composite loss factor for n^{th} mode can be calculated by

$$\eta_m = \frac{\phi_m^T [K_{nI}] \phi_m}{\phi_m^T [K_{nR} + K_{gn}] \phi_m} \quad (27)$$

Where $[K_{nR}]$ and $[K_{nI}]$ are the real and imaginary parts of the stiffness matrices for n^{th} harmonics respectively and ϕ_m is m^{th} axial mode eigenvector.

3 Results and discussion

Buckling and free vibration analysis of sandwich general shells of revolution under thermal environment for different geometry and also for different composite facings, viscoelastic core (EC2216 and DYAD606) materials is investigated. The temperature over the shell structure is assumed to be constant. The variation of frequency and loss factor for different core to facing (t_c/t_f) thickness ratio, length to mean radius (L/R) ratio in case of truncated conical shell and radius to total thickness (R/t) ratio in case of hemi spherical shell with cut out at a apex, $t = (2t_f + t_c)$, under clamped-clamped (C-C) boundary condition are studied. The variation of shear modulus and loss factor with temperature for two types of cores is reported by Nashif, Jones and Henderson (1985) are shown in figure 2.

3.1 Validation

The sandwich shells with orthotropic facings and viscoelastic core under thermal environment are not available in the literature. In order to ensure the correctness of the code developed in the present study, the frequency and loss factor are validated with sandwich cylindrical shell with isotropic facing and viscoelastic core presented by Pradeep, Ganesan and Padmanabhan (2006). This has been carried out by converting the general shell in to cylindrical shell by changing R_ϕ equal to infinity, R_θ equal to R (radius), ϕ=90° and fiber angle=0.

The variation of frequency and loss factor with temperature obtained from Pradeep, Ganesan and Padmanabhan (2006) are shown in figure 3, and the corresponding results of the present formulation are given in figure 4. Comparing the figure 3 and 4 it can be seen that there is a very good agreement between the two formulations as for as the loss factor are concerned. In case of fundamental frequency slight variation is observed. This may be due to fact that, the present formulation is general shells of revolution using isoparametric three noded element with seven degrees of freedom per node applicable to Wilkins theory, but Pradeep, Ganesan and Padmanabhan (2006) are used the two noded element having six degrees of freedom per node applicable to thin shell theory. However there is a good agreement between the frequencies at higher modes, moreover the buckling temperature at fundamental mode is having good agreement with Pradeep, Ganesan and Padmanabhan (2006). The properties and geometry of the clamped-clamped cylindrical shell with EC2216 core used by Pradeep, Ganesan and Padmanabhan (2006) are tabulated in the table 1.

In order to validate the present formulation of sandwich shell with orthotropic facings under thermal environment, the results are taken at atmospheric temperature and validated with Ramasamy and Ganesan (1999). The geometry and material properties used for the validation are given in table 2.

Figure 5 shows the variation of frequency and loss factor with circumferential mode number, there is a very good agreement between the present results and reference (Ramasamy and Ganesan (1999)). Based on these validations, the present study extended to investigate the behaviour of sandwich truncated conical and hemispherical shells with composite facings and viscoelastic core under thermal environment.

3.2 Buckling and free vibration of truncated conical shell

The general shell element with sandwich structure, which is converted in to conical shell by making R_ϕ has infinity and cone angle $\alpha = 90 - \phi$, is shown in figure 6(a). Where L is length of the shell, $r = r(s) = a + s\sin\alpha$ is the radius at the coordinate point (s, θ, z), a and b are the small and big end radius of the conical shell respectively and mean radius $R = (a+b)/2$. The figure 6(b) shows the cross- sectional view of the shell thickness,

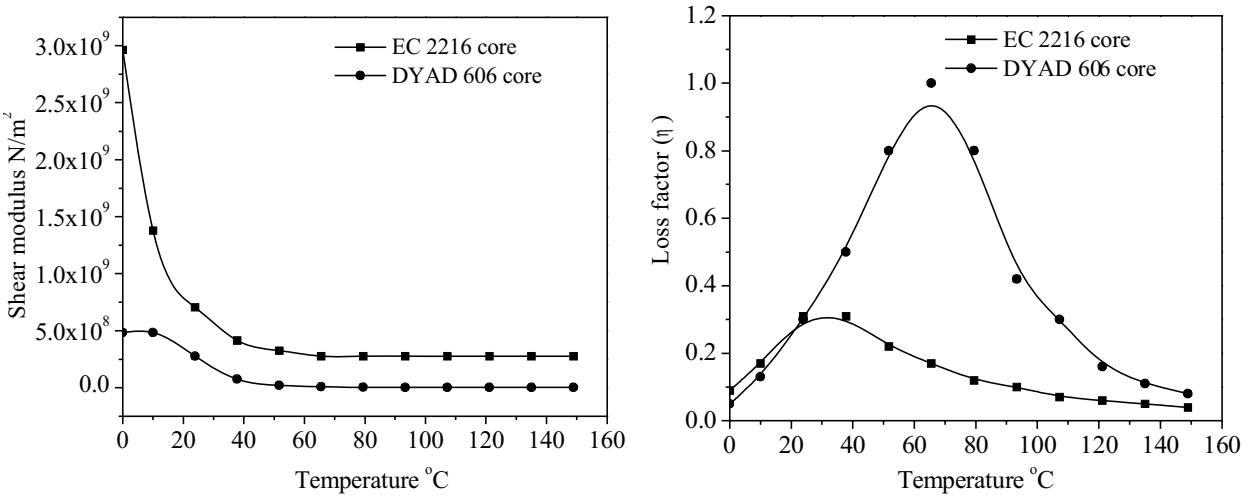

Figure 2: Shear modulus and Loss factor with temperature for EC2216 and DYAD606 core material (Nashif, Jones and Henderson 1985).

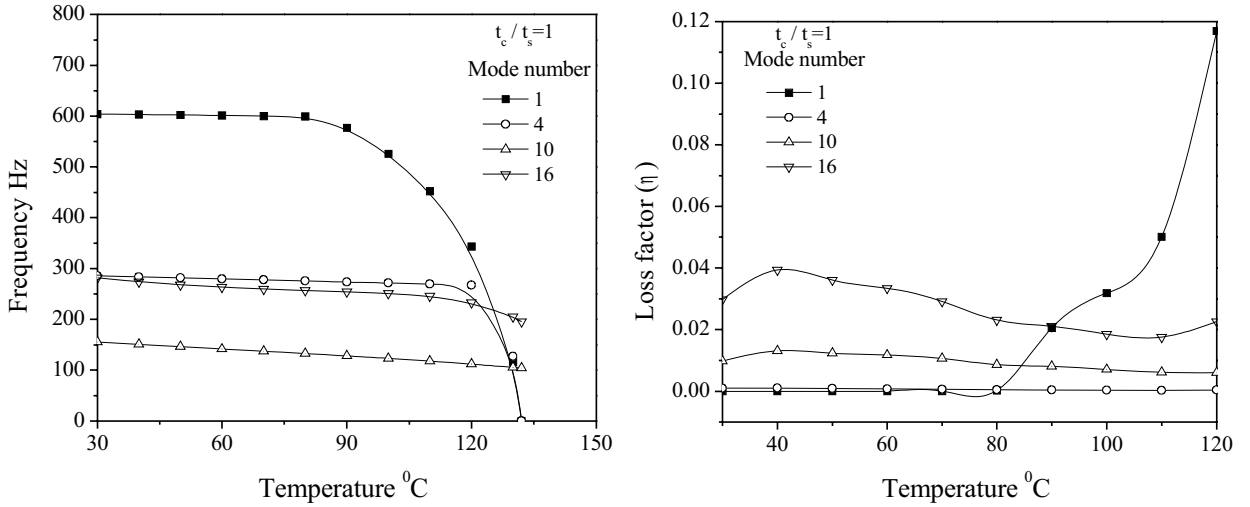

Figure 3: Frequency and modal loss factor with temperature (Pradeep, Ganesan and Padmanabhan (2006)).

Table 1: Properties and geometry proposed by Pradeep, Ganesan and Padmanabhan (2006)

E=206GPa, ν_s=0.3, ρ_s=7800kg/m^3, G^*_{core}=620.5(1+0.3i)$_{T=30}$MPa, ρ_{core}=1340kg/m^3, Length=L=1m, Radius=R=1m, Thickness=t_c=t_s=1.5mm

Table 2: Properties and geometry proposed by Ramasamy and Ganesan (1999)

E_1=76GPa, E_2=5.5GPa, G_{12}=2.3GPa, ν_s=0.34, ρ_s=1460kg/m^3, G^*_{core}=23(1+0.34i)$_{T=30}$MPa, ρ_{core}=1340kg/m^3, Length=L=12.2m, Radius=R=18.29m,Thickness=t_c=t_s=0.0127m

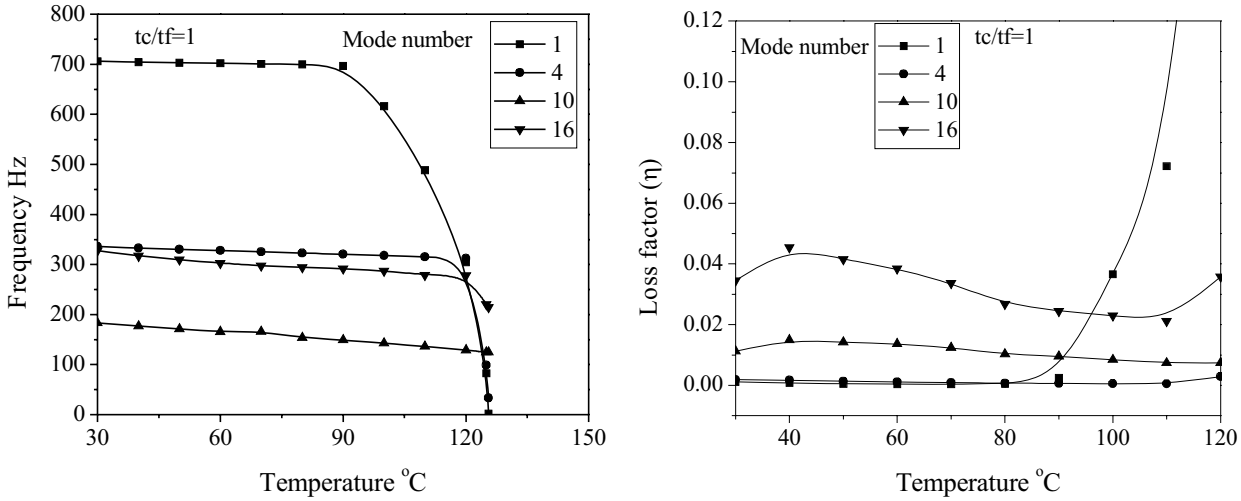

Figure 4: Frequency and loss factor with buckling temperature for EC2216 core sandwich cylindrical shell.

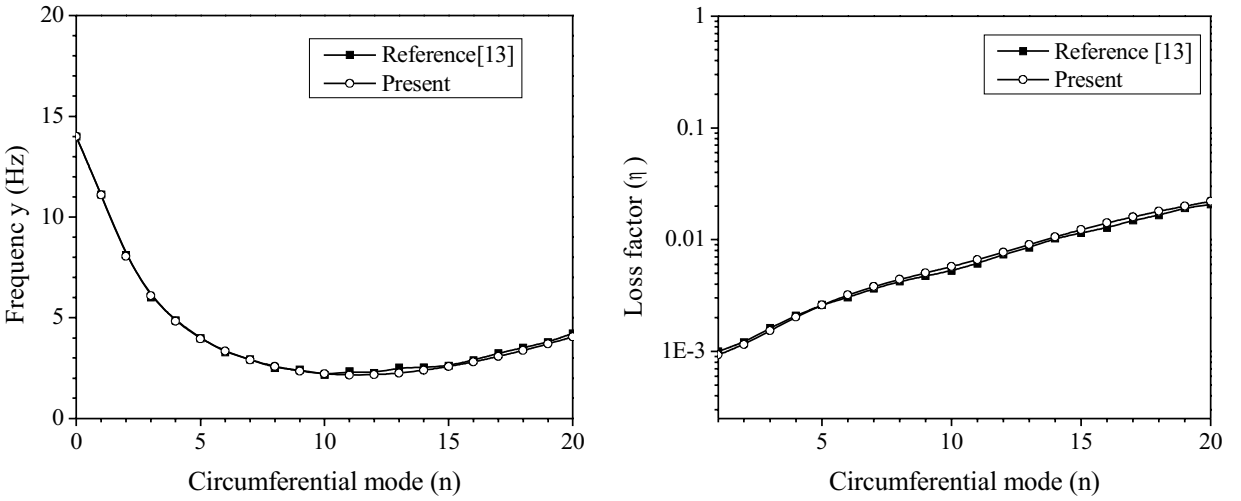

Figure 5: Validation with Ramasamy and Ganesan (1999), t_c/t_f=1,kevelar/epoxy composite cylindrical shell.

where t_f and t_c are the facings and core thickness respectively.

Buckling and free vibration analysis of sandwich conical shell by using general shell element under thermal environment is investigated. There are three types of composite facings such as graphite/epoxy, glass/epoxy and boron/epoxy are used in the present study and the detail study has been conducted on boron/epoxy composite facings with different core materials.

The material properties used in the present study are listed in the table 3 are reported by Jones (2005). Two types of cores such as EC2216 and DYAD606 are used for the present analysis by taking in to account of temperature independent and dependent shear modulus of the cores. The complex shear moduli values considered in the present analysis for EC2216 and DYAD606 are 580 (1+0.3i) MPa and 187 (1+0.388i) MPa respectively at room temperature.

3.2.1 Buckling analysis of truncated conical shell

3.2.1.1 Effect of facing material on buckling temperature at different modes

Variation of buckling temperature of conical sand-

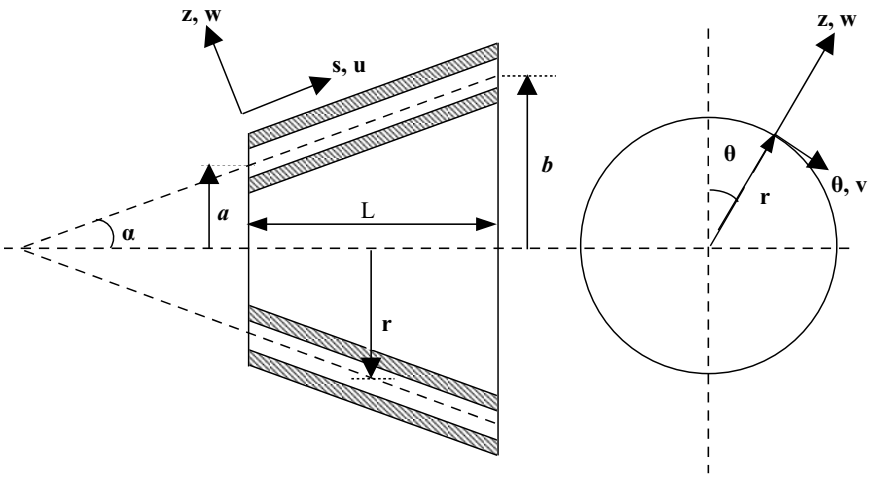

Figure 6(a): Geometry of a truncated conical sandwich shell

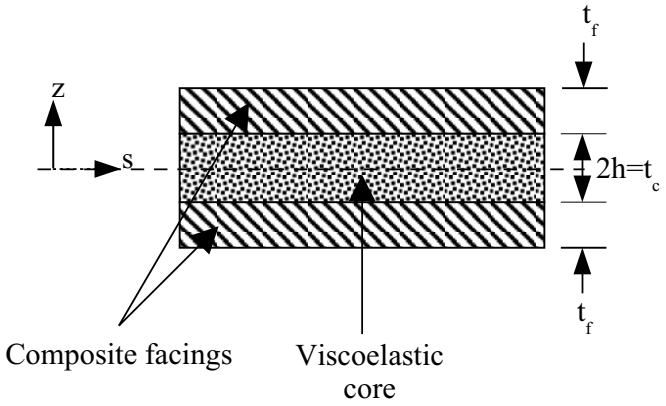

Figure 6(b): Cross-sectional view of shell thickness with composite facings and viscoelastic core.

Table 3: Composite lamina properties (Jones 2005)

Facing material	E_1 (GPa)	E_2 (GPa)	ν_{12}	G_{12} (GPa)	α_1 $(10^{-6}/^oC)$	α_2 $(10^{-6}/^oC)$
High-strength Graphite-epoxy (AS-3501)	128	11	0.25	4.5	0.45	27.4
E-Glass-epoxy	53.4	17.9	0.25	8.6	6.3	20.5
Boron-epoxy	204	18.5	0.23	5.6	6.1	30.3

wich shell with different composite facings and EC2216 core having cone angle 15° in clamped-clamped condition is investigated. Figure 7 shows the variation of buckling temperature with different circumferential modes. The buckling temperature decreases with increasing the mode number, there is a drastic reduction of buckling temperature up to n=10 then onwards more or less remains constant.

From the figure 7 it is observed that the graphite-epoxy sandwich conical shell is having very high buckling temperature compared to glass epoxy and boron-epoxy sandwich shells at all modes. This trend may be due to the co-efficient of thermal expansion of graphite-epoxy composite in fiber direction is very low compared to other two materials. Because of that the compressive stress developed in the graphite-epoxy composite sandwich shell is very low which leads to higher buckling temperature.

3.2.1.2 Buckling analysis of boron-epoxy sandwich conical shell

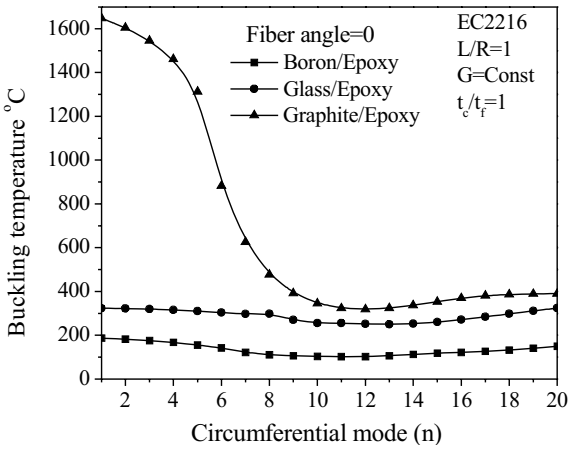

Figure 7: Buckling temperature with harmonics at zero fiber angle.

The glass-epoxy and graphite-epoxy composite facing conical shells are having very high buckling temperature, so that the viscoelastic material not with stand at high temperature. The detail study of sandwich conical shell with viscoelastic layer is carried out by using boron-epoxy composite facings, which is having lower buckling temperature compared to other two composite facing materials. In the study of boron-epoxy sandwich conical shell, composite damping is not included.

a) Effect of core to facing thickness ratio on buckling temperature

Figure 8 shows the first axial mode buckling temperature for first 20 circumferential modes of a truncated conical shell with EC2216 core and boron-epoxy composite facings in clamped-clamped (C-C) condition, by taking the fiber angle 0°, cone angle as 15° and length to mean radius ratio (L/R) as 1. From the figure 8 it is noticed that the buckling temperature decreases with increasing the circumferential mode and reaches a minimum value then onwards starts increasing with circumferential modes. The buckling temperature increases with increase in core thickness at all the modes, which is observed in both cases, when shear modulus (G^*) of the core considered as a function of temperature and independent of temperature. Doubling the core thickness there is an increase in the buckling temperature by about 50 to 75°C at lower and higher modes. Figures 8(a) and 8(b) show the variation of buckling temperature with circumferential modes for EC2216 core by considering the shear modulus constant (at room temperature) and function of temperature respectively. Comparing the figures 8(a) and 8(b) it is noticed that the buckling temperature of the structure is more when the G^* is constant with temperature at room temperature.

In reality, the shear modulus is function of temperature, the variation of shear modulus of the EC2216 with temperature shown in figure 2 is given by Nashif, Jones and Henderson (1985). The shear modulus decreases with temperature due to that the buckling temperature of the structure is lower, when the shear modulus considered as a function of temperature.

b) Effect of core material on buckling temperature

Figure 9 shows the first axial mode buckling temperature of conical sandwich shell with DYAD606 core material by considering the temperature independent and dependent shear modulus of the core. From the figure 9(a) it is noticed that the buckling temperature follows the same pattern of curves of EC2216 core sandwich conical shell with harmonics. The buckling temperature increases with increase in core thickness at all modes, which is observed when the constant shear modulus is considered at room temperature. Figure 9(b) shows the variation of buckling temperature with circumferential modes when the temperature dependent shear modulus of DYAD606 core is considered. The buckling temperature decreases slightly with increasing the circumferential mode number, and also influence of core thickness on buckling temperature is not observed much. From the reference (Nashif, Jones and Henderson (1985)) it is observed that the shear modulus of DYAD606 after 50°C temperature becomes 1/10 the value of G^* at room temperature, because of that increasing the core thickness is not having effect on the buckling temperature.

Comparing the figure 9(a) and 9(b) it is observed that the buckling temperature is very low when the temperature dependent shear modulus of the core is considered. The reason for this is shear modulus of DYAD606 decreases drastically with temperature as reported by Nashif, Jones and Hen-

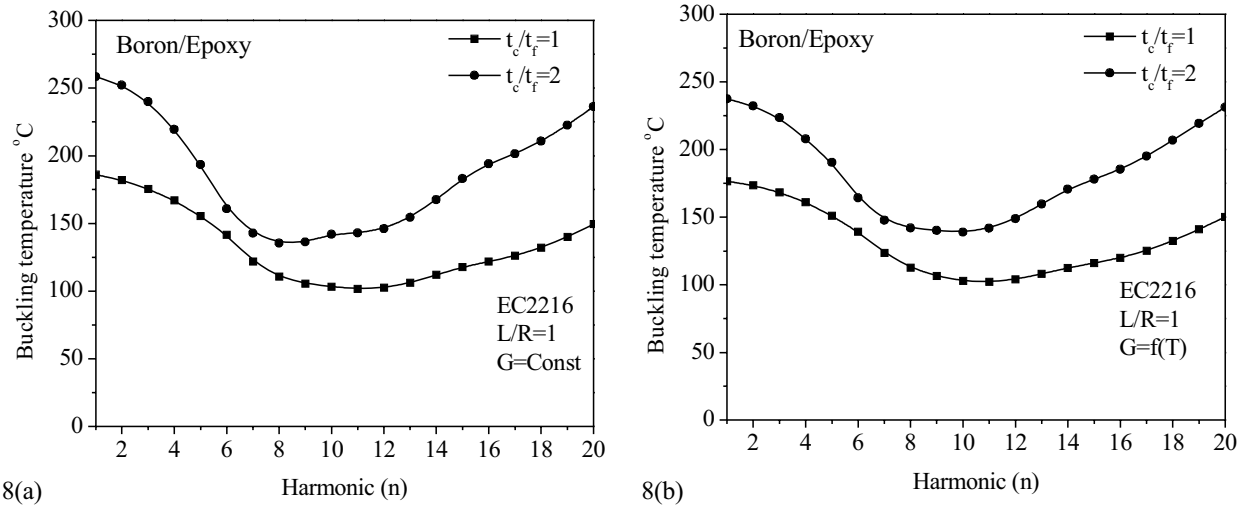

Figure 8: Buckling temperature of sandwich conical shell with boron/epoxy facings and EC2216 core material at zero fiber angle (a) G=Const,(b) $G = f(T)$.

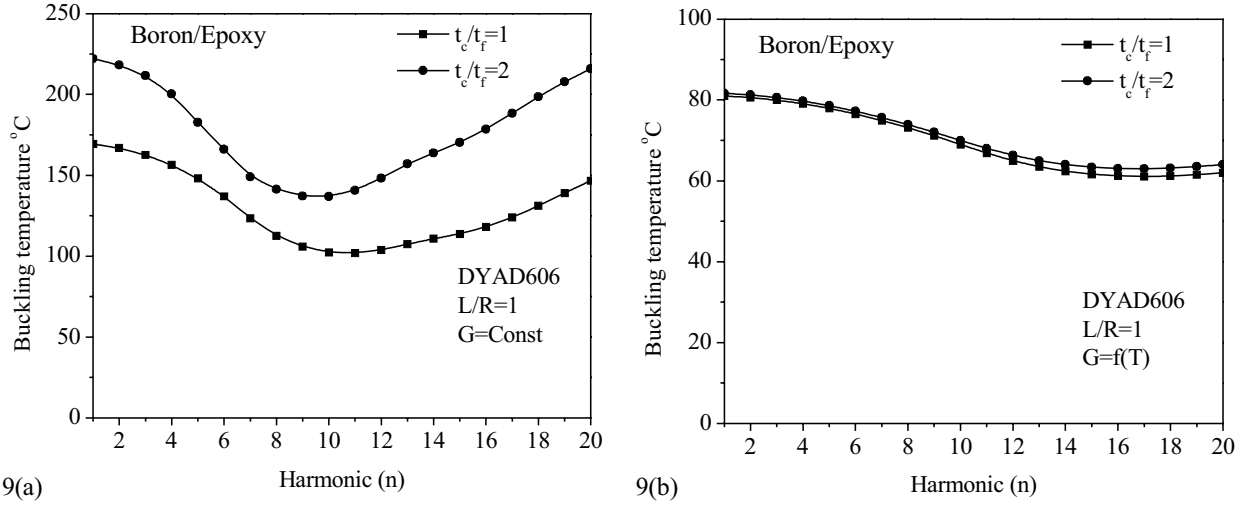

Figure 9: Buckling temperature of sandwich conical shell with boron/epoxy facings and DYAD606 core material at zero fiber angle (a) G=Const,(b) $G = f(T)$.

derson (1985, figure 2). Comparing the figure 8 and 9 the buckling temperature of conical sandwich shell with EC2216 core is having more than the DYAD606 core. In the present study the shear moduli values for EC2216 and DYAD606 core are 580MPa and 127MPa respectively, at room temperature. When these values are used for the analysis of the shell having EC2216 as core material has higher buckling temperatures than DYAD606 core material for any given thickness of the core. From reference (Nashif, Jones and Henderson 1985) (figure 2) it is found that when the temperature dependent shear modulus for DYAD606 is considered, the modulus falls drastically with temperature and becomes almost 1/10 of its value at room temperature for 20°C temperature rise. Where as in case of EC2216 core shear modulus does not change that much drastically. It only becomes 1/2 of its value at room temperature for the same temperature rise.

The truncated conical shell with EC2216 core material has a higher buckling temperature when the temperature dependent shear modulus is used for any given core thickness. It can be concluded

from these results that if the shear modulus of the core is high then the buckling temperatures will be high and also an increase in the core thickness considerably increases the buckling temperatures. In contrast when the shear modulus of core is low the buckling temperatures are lower and increase in core thickness has little influence on buckling temperature.

c) Effect of fiber orientation on buckling temperature

Figure 10 shows the variation of buckling temperature with fiber angle of a boron-epoxy composite facing sandwich conical shell having EC2216 and DYAD606 core materials at $m = n = 1$. Buckling temperature increases with increase in fiber angle in case of both the type of cored sandwich conical shells, and also increase in core to facing thickness ratio the buckling temperature increases. Increasing the fiber angle from 0 to 90 the stresses developed in clamped-clamped shell goes on decreases, which leads to increase in the buckling temperature of the shell.

The lowest buckling temperature of sandwich conical shell with EC2216 core at different fiber orientation of a circumferential (n) and axial (m) mode are tabulated in Table 4. From the table 4 it is noticed that the lowest buckling temperature of a truncated conical shell is observed at zero fiber orientation of 11^{th} circumferential mode.

Table 4: Lowest buckling temperature of sandwich conical shell with boron-epoxy facings and EC2216 core

Fiber orientation(degrees)	Buckling temperature ˚C (m, n)
0	101.9 (1,11)
15	125.9 (1,10)
30	264.4 (1,1)
45	424.9 (1,13)
60	332.2 (1,16)
75	295.2 (1,17)
90	539.8 (1,20)

m=Axial mode, n=Circumferential mode

3.2.2 Frequency and damping analysis of truncated conical shell

3.2.2.1 Influence of facing material on frequency and loss factor with temperature

Figure 11 shows the variation of frequency and loss factor with temperature, the study has been carried out up to 250˚C because viscoelastic layer cannot withstand at higher temperature. From the figure it is noticed that at atmospheric temperature glass-epoxy composite sandwich conical shell is having higher frequency than the other two composite sandwich conical shells. Increasing the temperature the frequency of boron-epoxy sandwich conical shell decreases, near the buckling temperature there is a drastic reduction in the frequency and finally approaches to zero at buckling temperature.

This may be due to increase in temperature in the equation (26) the real part of the stiffness $[K_R]$ reduces by the influence of geometric stiffness matrix $[K_g]$. Near the buckling temperature the stiffness of the structure becomes zero, due to the fact that the frequency attains to zero. Loss factor of sandwich conical shell with EC2216 core and boron-epoxy facing material is lower than other two facing (graphite-epoxy and glass-epoxy) materials at room temperature, as the temperature approaches the buckling temperature the loss factor value shoots up.

3.2.2.2 Influence of facing material on frequency at different harmonics

Figure 12(a) and 12(b) shows the variation of frequency with circumferential modes of conical sandwich shell with EC2216 core having glass-epoxy and graphite-epoxy composite facings respectively at 0˚ and 90˚ fiber orientation. Frequency decreases with increase in mode number and reaches a minimum value then increases with increase in mode number. At lower modes membrane energy is predominant with increase in mode number membrane energy reduces and frequency decreases, at higher modes bending energy is predominant which leads to increase in frequency with increasing the mode number after n=10.

In both type of composite facing materials, the

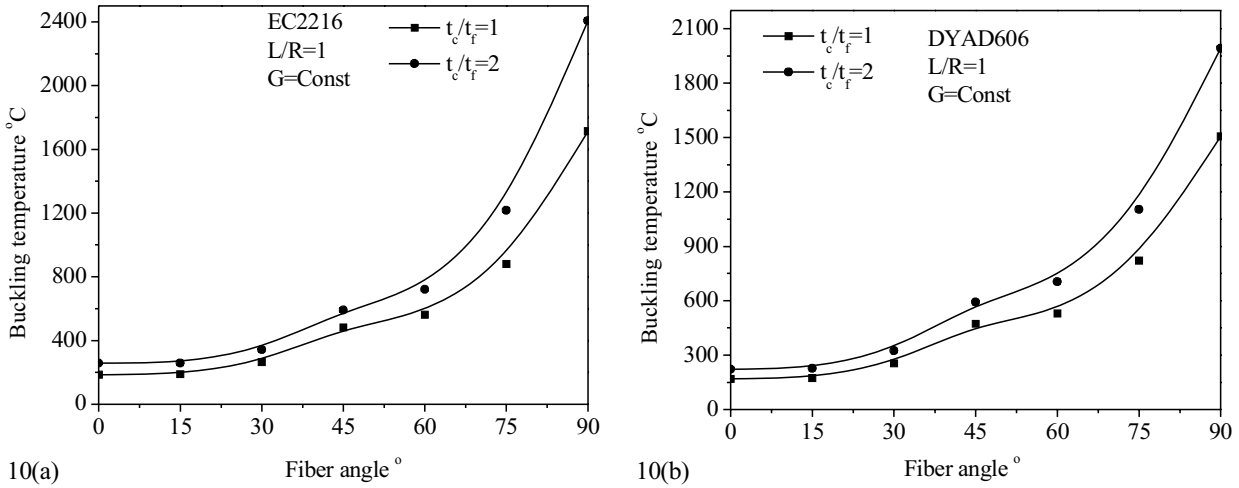

Figure 10: Variation of buckling temperature with fiber angle (a) EC2216 core (b) DYAD606 core.

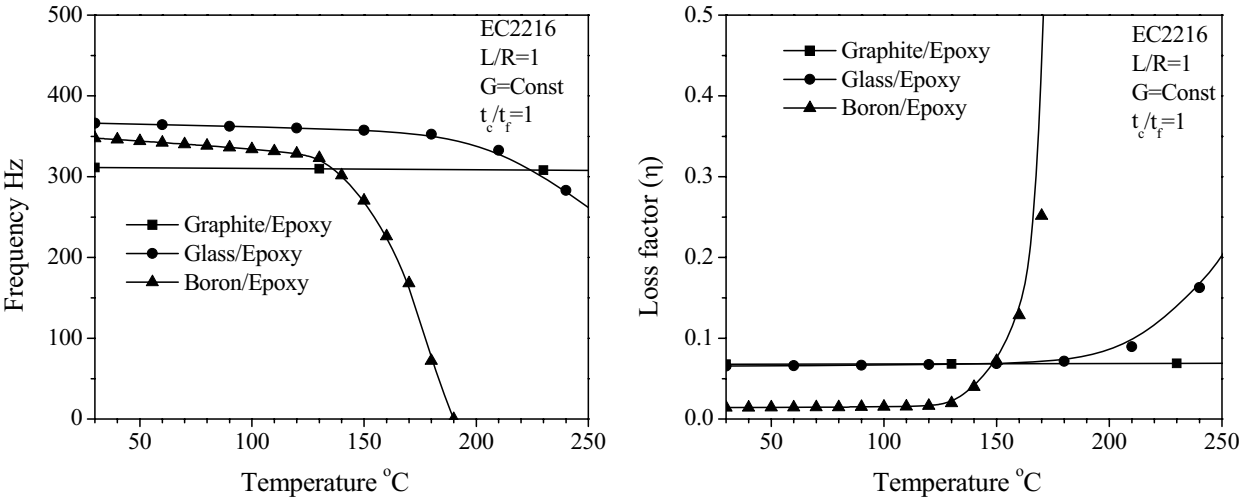

Figure 11: Frequency and loss factor with temperature at zero fiber orientation.

frequency at 90˚ fiber orientation is more compared to zero fiber orientation. The stiffness of the shell in circumferential direction is more when the fibers oriented at 90˚, which leads to increase in the frequency of the shell.

3.2.2.3 Influence of composite damping on total damping

Composite damping is the property of material and is obtained from the experiment. Composite damping also comes under Structural damping. Figure 13 shows the contribution of composite damping and viscoelastic (EC2216) damping to the total damping of the system. Figure 13(a) and 13(b) shows the variation of loss factor with circumferential modes for conical sandwich shell with EC2216 core having glass-epoxy and graphite-epoxy composite facings respectively at zero fiber orientation. From the figure 13(a) it is noticed that the composite damping is more than the viscoelastic damping at all the harmonics. Composite damping increases at lower modes and then decreases up to n=10 then onwards almost remains constant with increase in mode number. Viscoelastic damping decreases with increase in harmonics. Comparing the figure 13(a) and 13(b) viscoelastic damping is more at lower modes when graphite-epoxy composite facings are used, which results in increase in total damping of the sandwich conical shell with graphite-epoxy com-

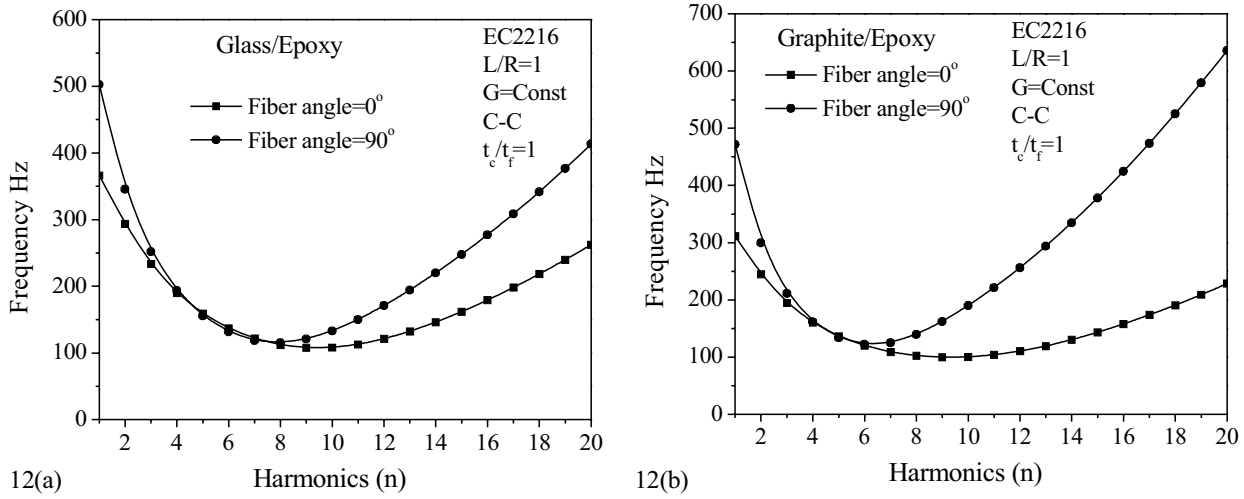

Figure 12: Frequency variation with circumferential modes for different fiber orientation (a) Glass/Epoxy (b) Graphite/Epoxy.

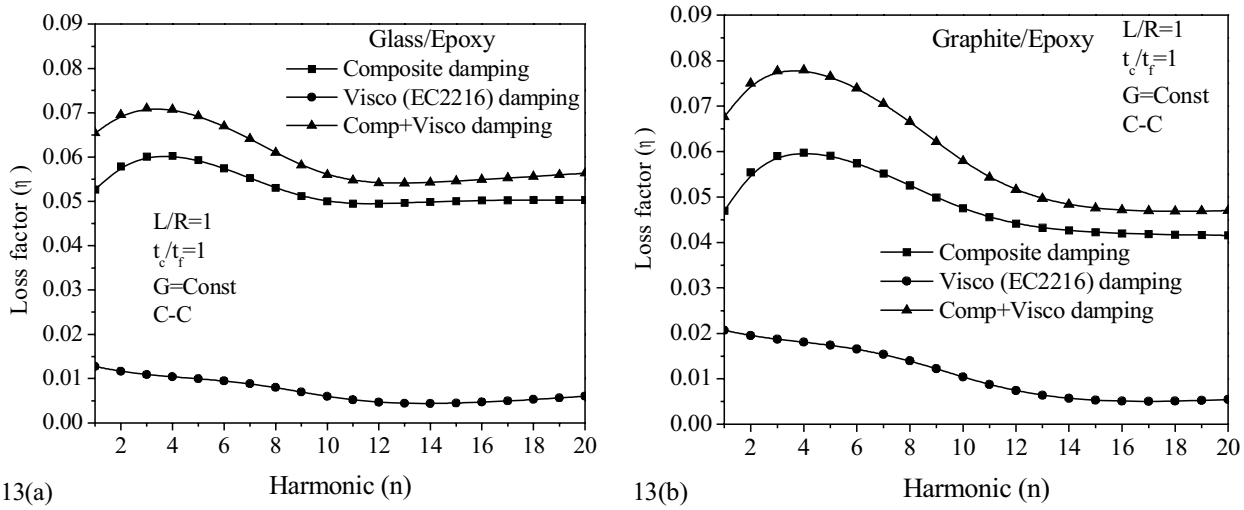

Figure 13: Effect of composite damping on total damping at zero fiber orientation (a) Glass/Epoxy (b) Graphite/Epoxy.

posite facings.

Similarly as discussed above the figure 14(a) and 14(b) shows the variation of loss factor at 90˚ fiber orientation. From the figure 14 it is observed that when the fiber orientation is at 90˚ the composite damping is more predominant in lower modes and viscoelastic damping is dominant at higher modes. It is advantages to use both composite and viscoelastic damping so that the vibrations can be controlled either the system vibrate at lower or higher modes. Comparing the figure 13 and 14 the total damping at higher modes is more at zero fiber orientation.

3.2.2.4 Frequency and damping analysis of boron-epoxy sandwich conical shell

Frequency and damping analysis of boron-epoxy composite facings sandwich conical shell with cone angle (α) 15˚ and fiber angle 0˚ in clamped –clamped condition is carried out. Parametric studies are considered as different core material with temperature dependent and independent shear modulus of the core.

a) Variation of frequency and loss factor with tem-

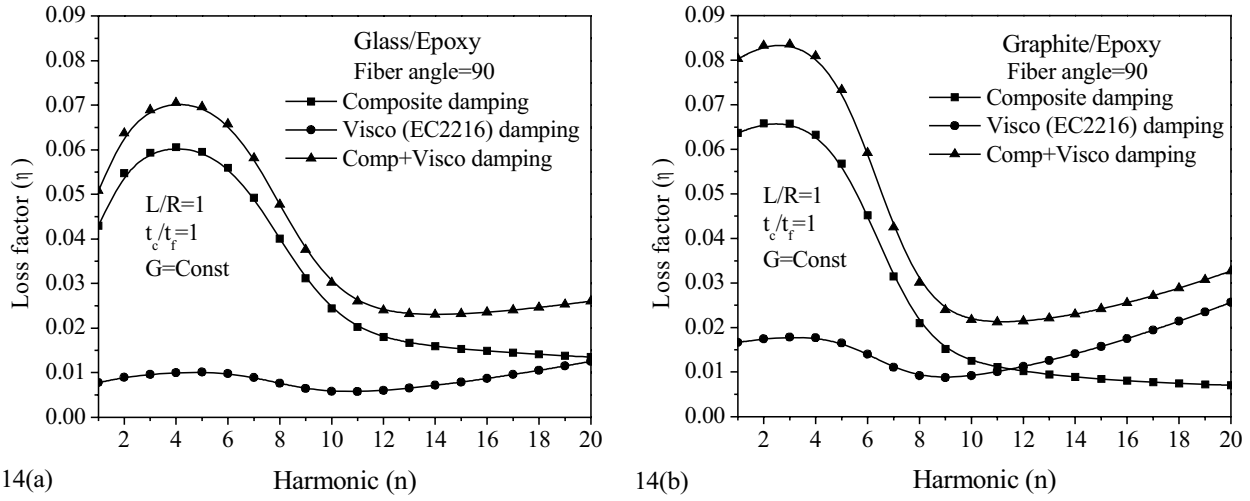

Figure 14: Effect of composite damping on total damping at 90° fiber orientation (a) Glass/Epoxy (b) Graphite/Epoxy.

perature

Figure 15 shows the variation of frequency and loss factor with buckling temperature for different circumferential modes. The core material EC2216 with t_c/t_f ratio 1 and L/R ratio 1, the shear modulus of the core assumed to be constant with temperature. The natural frequency of the shell decreases slightly with increase in temperature till the temperature is closer to the buckling temperature. When the buckling temperature is approached, the frequency falls very sharply with the increase in temperature and finally tends to zero at critical buckling temperature of a particular mode. Since the buckling temperatures of the higher modes are lower, so the frequency of higher modes becomes zero before the first mode buckling temperature.

The loss factor of the shell for all modes remains constant up to certain temperature and then start to increase with temperature reaching a very high value when temperature approaches the buckling temperature of particular modes. This is expected because the denominator value in the equation (27) decreases as the temperature increases due to the effect of $[K_{gn}]$ matrix, which leads to increase in the loss factor of the shell.

b) Influence of core material on frequency

Figure 16 shows the variation of frequency and modal loss factor of a sandwich conical shell with temperature for DYAD606 core material. The variation of frequency and loss factor with temperature are similar trend as compared to conical shell having EC2216 core material (figure 15). Comparing the figure 15 and 16 it is observed that the conical shell with DYAD606 core is having lower buckling temperatures for given core thickness. From the reference (Nashif, Jones and Henderson 1985) (figure 2) it is observed that the shear modulus of DYAD606 core is lower than the EC2216, due to fact that the stiffness of conical shell with DYAD606 core is lower than the EC2216 core, so the DYAD 606 core sandwich conical shell frequency attains to zero and loss factor shoots up earlier than the EC2216 core due to lower buckling temperature.

c) Influence of temperature dependent properties of core material:

Figure 17 shows the variation of natural frequency and loss factor for a sandwich conical shell with EC2216 core material. The shear modulus of the core is considered as a function of temperature (variation of shear modulus with temperature of EC2216 and DYAD606 are given in figure 2). The frequency and loss factor pattern is similar as explained in the earlier section 3.2.2.4(a), when temperature independent shear modulus is used. Comparing the figure 15 and 17 there is a slight

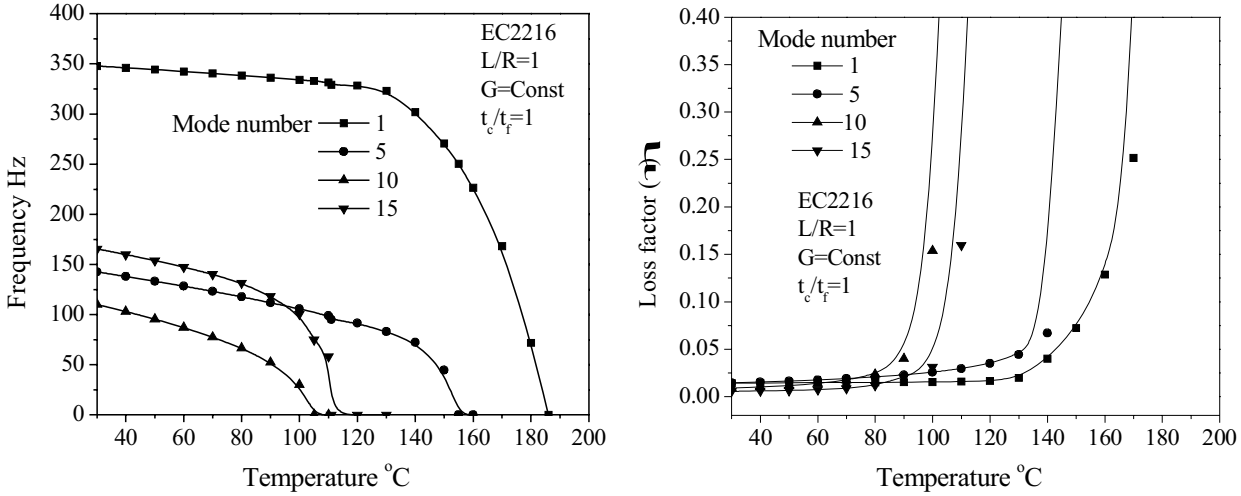

Figure 15: Frequency and loss factor with temperature for EC2216 core having G=const

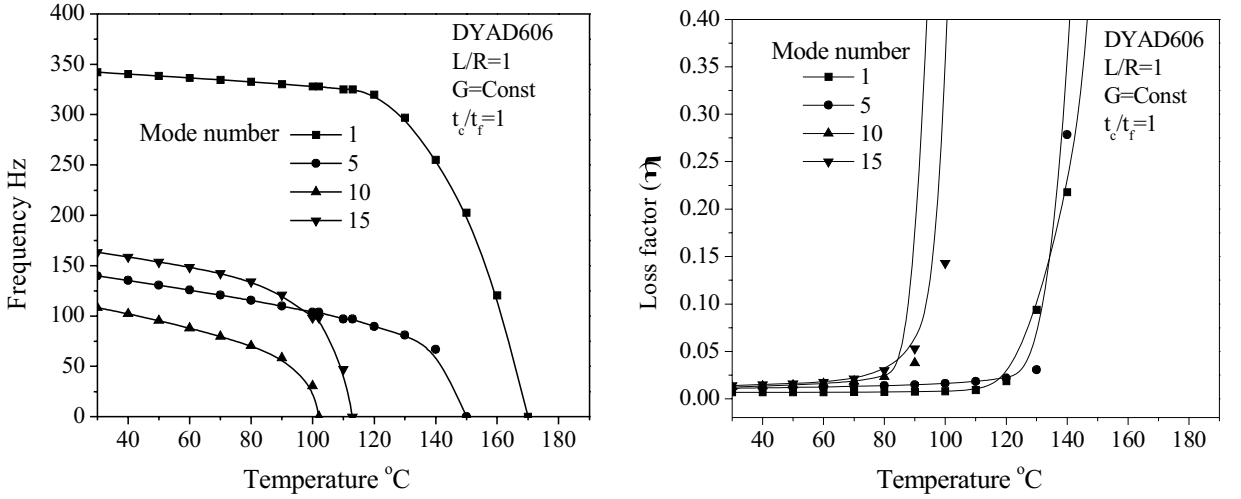

Figure 16: Frequency and loss factor with temperature for DYAD606 core having G=const

change in the buckling temperature at which frequency becomes zero. As the temperature approaches the buckling temperature the loss factor start increasing and tends to a high value near the buckling temperature.

d) Variation of frequency and loss factor with fiber angle for different modes

Figure 18 shows the variation of frequency and loss factor with fiber orientation of a boron-epoxy facing and EC2216 core sandwich conical shell. Shear modulus of the core considered as constant and core to facing thickness ratio (t_c/t_f) 1, length to mean radius ratio (L/R) 1, in clamped-clamped condition at atmospheric temperature. From figure 18 it is observed that first fundamental mode frequency increases with increasing the fiber orientation and the frequency of higher modes are lower than the fundamental mode at any fiber orientation. Loss factor remains constant with fiber orientation at fundamental mode but at higher modes loss factor increases with fiber angle.

Figure 19 shows the variation of frequency and loss factor with fiber orientation of a boron-epoxy facing and DYAD606 core sandwich conical shell. Comparing the figure 18 and 19 there no much difference observed in the frequency trend but the loss factor of sandwich shell with DYAD606 core is having more damping than

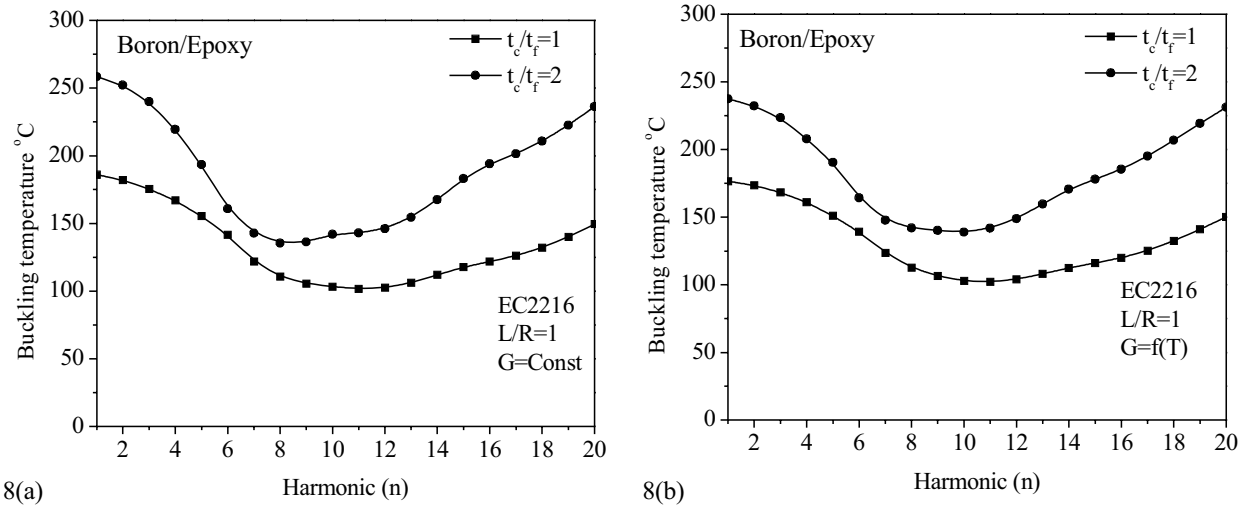

Figure 17: Frequency and loss factor with temperature for EC2216 core having $G = f(T)$

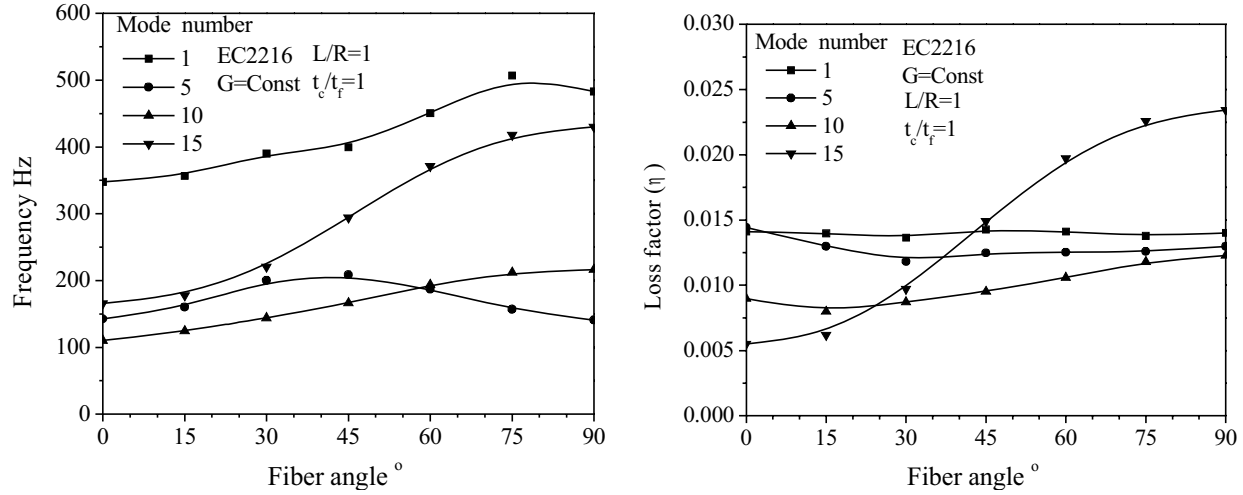

Figure 18: Frequency and loss factor with fiber angle for different modes of sandwich conical shell with EC2216 core.

EC2216 core which is observed at 90° fiber orientation. Comparing the figure 19 and 20 increasing the L/R ratio frequency and loss factor decreases, which are observed at all fiber orientation. Increasing the L/R ratio the mass of the structure increases which leads to decrease in the frequency.

3.3 Buckling and free vibration of hemispherical shell with cut out at apex

The study has been extended to some typical cases of hemispherical shell with boron-epoxy facings and EC2216 core having 15° cut out angle (β) at apex as shown in figure 21. The parametric study is carried out for different radius to total thickness (R/t) ratio, core to facing thickness ratio (t_c/t_f) and various fiber orientations. The general shell element, which is also converted in to hemispherical shell by making R_ϕ and R_θ equal to radius R as shown in Figure 21. Where β is the cut out angle at apex, the mid surface is discretised in to finite elements is also shown in figure 21.

3.3.1 Buckling analysis of hemispherical shell

Figure 22(a) shows the variation of buckling temperature with circumferential modes (n) by considering the temperature independent shear mod-

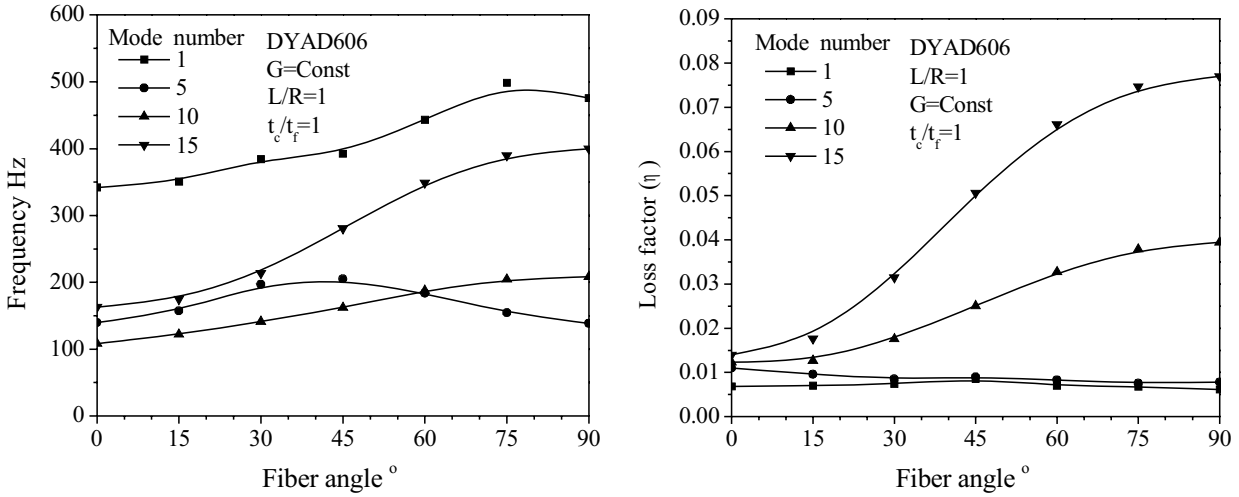

Figure 19: Frequency and loss factor with fiber angle for different modes of sandwich conical shell with DYAD606 core.

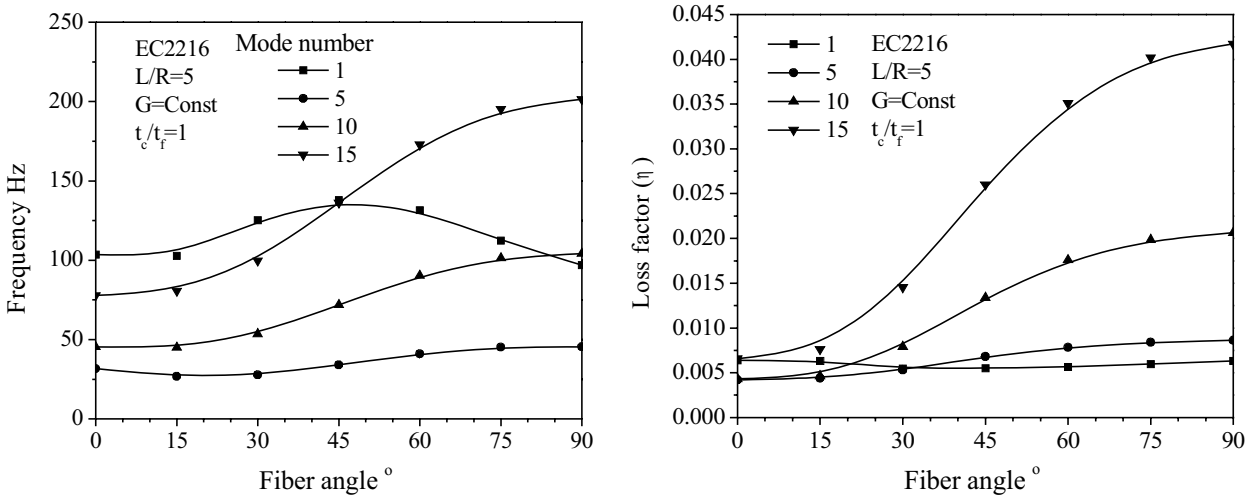

Figure 20: Frequency and loss factor with fiber angle for different modes of sandwich conical shell with EC2216 core $L/R = 5$

ulus of the core. Buckling temperature increases with circumferential modes up to n=5 and reaches a very high value then decreases with increasing the circumferential modes. Buckling temperature increases with increasing the core to facing thickness ratio, which is observed at all the harmonics. Increasing the core thickness two times there is increase in buckling temperature about 100˚C, which is observed at fundamental mode (n=1). Figure 22(b) shows the variation of buckling temperature with fiber angle for different harmonics by considering shear modulus of the core constant with temperature. Buckling temperature of 5^{th} harmonic is more compared to other lower and higher harmonics at all fiber orientation. Buckling temperature increases with fiber angle up to 30˚ then onwards decreases with increasing the fiber angle.

3.3.2 Free vibration analysis of hemispherical shell

The buckling temperature of sandwich hemispherical shell is more than the sandwich conical shell, the viscoelastic core is not withstanding at higher temperature because of that the frequency study is limited to 200˚C. Figure 23 shows the

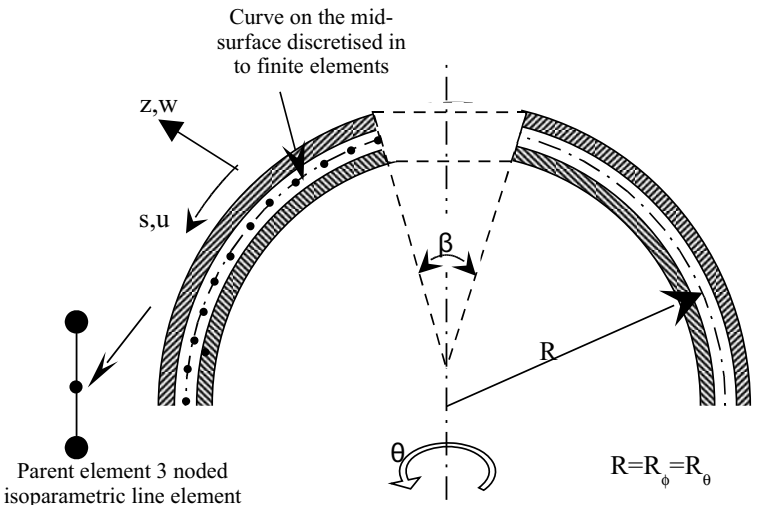

Figure 21: Cut section of hemispherical shell with cut out angle at apex.

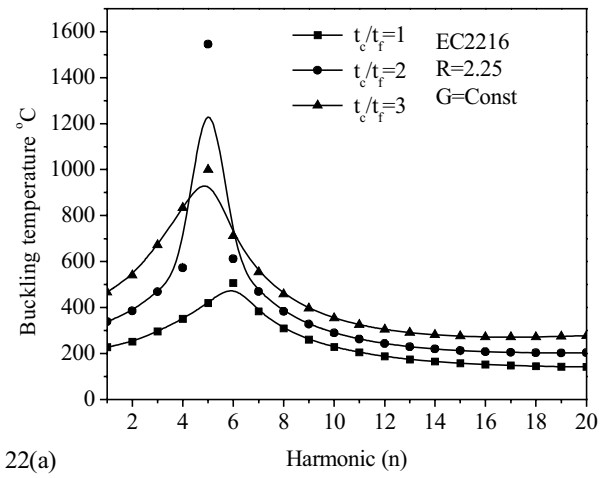

Figure 22(a): Buckling temperature with harmonics for various core to facing thickness ratio (t_c/t_f).

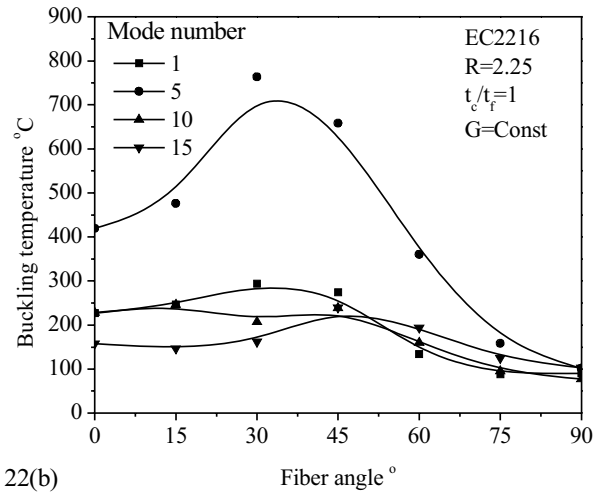

Figure 22(b): Buckling temperature with fiber angle for different harmonics (n).

variation of frequency and loss factor with temperature for different radius to total thickness ratio (R/t) at zero fiber orientation. Frequency increases with increasing the temperature at lower modes (n=1) but at higher modes (n=5) frequency decreases with increase in temperature. Loss factor decreases with increasing the temperature at lower modes (n=1) but at higher modes (n=5) loss factor increases with increasing the temperature.

This trend may be due to at lower modes membrane effect is more and when the mode number increases bending effect becomes predominant. Decreasing the R/t ratio frequency and loss factor increases at all the temperature which is observed at n=1.

Figure 24 shows the variation of frequency and loss factor with fiber orientation for different radius to total thickness ratio (R/t) at atmospheric temperature. From the figure 24 it is observed that frequency increases with increasing the fiber angle at lower modes (n=1), and at higher modes (n=5) frequency increases up to 30° fiber orientation then onwards decreases with increasing the fiber angle. Loss factor decreases with increas-

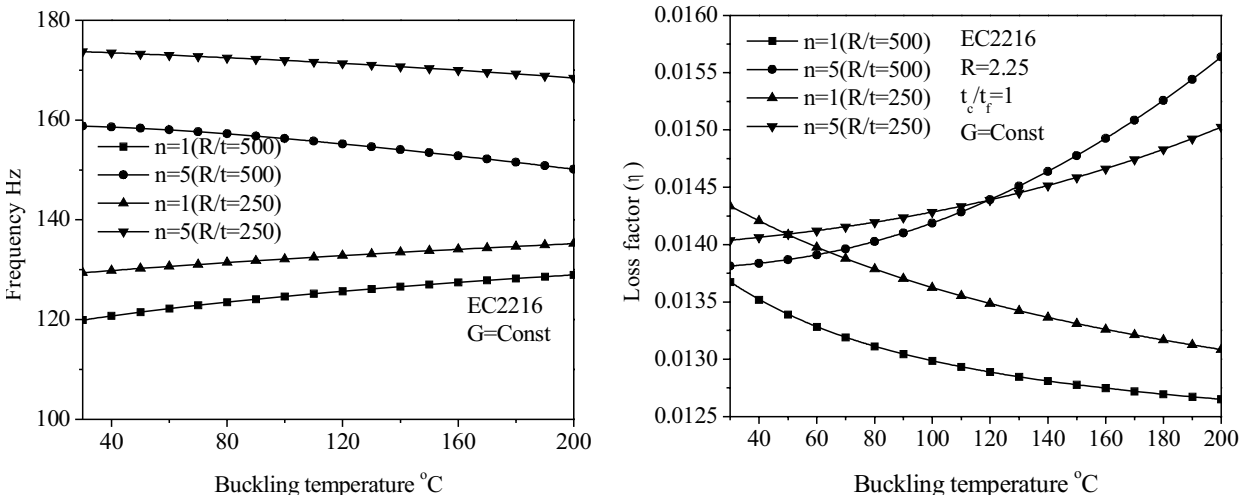

Figure 23: Variation of frequency and loss factor with temperature for different radius to total thickness (R/t) ratio.

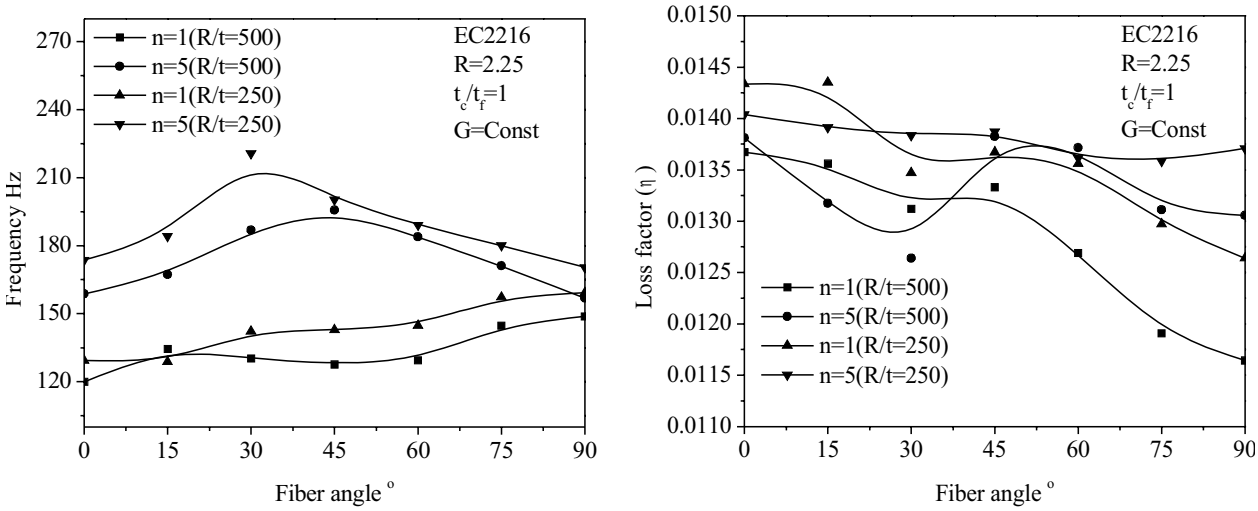

Figure 24: Variation of frequency and loss factor with fiber angle for different R/t ratio.

ing the fiber angle which is observed at n=1. Decreasing the radius to total thickness (R/t) ratio frequency and loss factor increases at all fiber orientation at n=1.

4 Conclusions

The buckling and free vibration analysis of sandwich general shells of revolution under thermal environment is investigated for different geometry such as truncated sandwich conical shell and hemispherical shell with cut out at apex using various facing and core materials. The following conclusions are obtained from the investigation.

1. The graphite-epoxy sandwich truncated conical shell is having very high buckling temperature compared to glass epoxy and boron-epoxy sandwich shells at all modes. This trend may be due to the co-efficient of thermal expansion of graphite-epoxy composite in fiber direction is very low compared to other two materials.

2. In case of glass epoxy and graphite-epoxy composite facing materials the frequency at 90° fiber orientation is more compared to zero fiber orientation. The stiffness of the conical shell in circumferential direction is

more when the fibers oriented at 90˚, which leads to increase in the frequency of the conical shell.

3. The composite damping is more than the viscoelastic damping at all the harmonics. Viscoelastic damping is more at lower modes when graphite-epoxy composite facings are used, which causes increase in total damping of the sandwich conical shell compared to glass-epoxy composite facings.

4. Truncated sandwich conical shell buckling temperature increases with increase in core (EC2216) thickness at all modes, which is observed in both cases, when shear modulus (G^*) of the core considered as a function of temperature and independent of temperature. Doubling the core thickness there is an increase in the buckling temperature by about 50 to 75˚C at lower and higher modes. Buckling temperature of the structure is more when the G^* is constant with temperature at room temperature.

5. The truncated sandwich conical shell with EC2216 core material has a higher buckling temperature compared to DYAD606 core when the temperature dependent shear modulus is used for any given core thickness.

6. The natural frequency of the conical shell decreases slightly with increase in temperature and near the buckling temperature frequency becomes zero at a particular mode. Since the buckling temperatures of the higher modes are lower, so the frequency of higher modes becomes zero before the first mode buckling temperature.

7. The loss factor of the conical shell for all modes remains constant up to certain temperature and then start to increase with temperature reaching a very high value when temperature approaches the buckling temperature of particular modes.

8. Hemispherical sandwich shell buckling temperature increases with circumferential modes up to n=5 and reaches a very high value then decreases with increasing the circumferential modes. Increasing the core thickness two times there is increase in buckling temperature about 100˚C, which is observed at fundamental mode (n=1). Decreasing the R/t ratio frequency and loss factor increases at all the temperature which is observed at n=1.

9. Hemispherical sandwich shell frequency increases with increasing the fiber angle at lower modes (n=1), loss factor decreases with increasing the fiber angle which is observed at n=1. Decreasing the radius to total thickness (R/t) ratio, frequency and loss factor increases at all fiber orientation at n=1.

References

Arthur, W. L.; Jae, H.K. (1999): Three-dimensional vibration analysis of thick shells of revolution. *J. of Eng Mechanics*, Vol. 125(12), pp. 1365-1371.

Arthur, W. L.; Jae, H. K. (2004): Three-dimensional vibration analysis of thick complete conical shells. *ASME J of Applied Mechanics,* Vol. 71, pp. 502-507.

Arthur, W. L.; Jae, H. K. (2005): Free vibrations of thick, complete conical shells of revolution from a three-dimensional theory. *ASME J of Applied Mechanics*, Vol. 72, pp. 797-800.

Baiz, P. M.; Aliabadi, M. H. (2006): Linear buckling analysis of shear deformable shallow shells by the boundary domain element method. *CMES: Computer Modeling in Engineering & Sciences.* Vol. 13, No. 1, pp. 19-34.

Bardell, N. S.; Langley, R. S.; Dunsdon, J. M.; Aglietti, G.S. (1999): An h-p finite element vibration analysis of open conical sandwich panels and conical sandwich frusta. *J. of Sound and Vibration*, Vol. 226(2), pp.345-377.

Bardell, N. S.; Langley, R.S.; Dunsdon J.M. (1998): Free vibration of thin, isotropic, open conical panels. *J. of Sound and Vibration*, Vol. 217(2), pp. 297-320.

Buchanan, G. R.; Wong, F.T.I. (2001): Frequencies and mode shapes for thick truncated hollow

cones. *Int. J. of Mechanical Sciences*, Vol. 43, pp. 2815-2832.

Chen, W. Q.; Ding, H. J. (2001): Free vibration of multi-layered spherically isotropic hollow spheres. *Int. J. of Mech Sci*, Vol. 43, pp. 667-680.

Chih, P. W.; Jyh, Y. L.; Jyh, K.C. (2005): A three dimensional asymptotic theory of laminated piezoelectric shells. *CMC: Computers*, *Materials & Continua* Vol. 2, No. 1, pp. 119-138.

Ching, H. K.; Chen, J. K. (2006): Thermomechanical analysis of functionally graded composites under laser heating by the MLPG method. *CMES: Computer Modeling in Engineering & Sciences.* Vol. 13, No. 3, pp. 199-217.

De Souza, V.C.M.; Croll, J.G.A. (1980): An energy analysis of the free vibrations of isotropic spherical shells. *J. Sound and Vibration*, Vol. 73(3), pp.379-404.

De Souza, V.C.M.; Croll, J.G.A. (1981): Free vibrations of orthotropic spherical shells. *Eng. Struct*, Vol. 3, pp. 71-84.

Gautham, B. P.; Ganesan, N. (1994): Vibration and damping characteristics of spherical shells with a viscoelastic core. *J. Sound and Vibration*, Vol. 170(3), pp. 289-301.

Jihan, K.; Yong, H. K.; Sung, W. L. (2004): Asymptotic postbuackling analysis of composite and sandwich structures via the assumed strain solid shell element formulation. *CMES: Computer Modeling in Engineering & Sciences.* Vol. 6, No. 3, pp. 263-276.

Jones, R. M. (2005): Thermal buckling of uniformly heated unidirectional and symmetric cross-ply laminated fiber-reinforced composite uniaxial in-plane restrained simply supported rectangular plates. *Composites: Part A*, Vol. 36, pp. 1355-1367.

Kadoli, R.; Ganesan, N. (2005): A theoretical analysis of linear thermoelastic buckling of composite hemispherical shells with a cut out at the apex. *Composite Struct*, Vol. 68, pp. 87-101.

Khatri, K. N. (1996): Antisymmetric vibration of multilayered conical shells with constrained viscoelastic layers. *Int. J. Solids Struct*, Vol. 33(16), pp.2331-2355.

Khatri, K. N.; Asnani, N. T. (1996): Vibration and damping analysis of fiber reinforced composite material conical shells. *J. of Sound and Vibration*, Vol. 193(3), pp. 581-595.

Khatri, K. N.; Asnani , N. T. (1995): Vibration and damping analysis of multilayered conical shells. *Composite Struct*, Vol. 33, pp. 143-157.

Li, J.; Xiang, Z. H.; Xue, M. D. (2005): Three-dimensional finite element analysis of honeycomb sandwich composite shells with cutouts. *CMC: Computers*, *Materials & Continua* Vol. 2, No. 1, pp. 139-150.

Liyong, T. (1993): Free vibration of composite laminated conical shells. *Int. J. Mech Sci*, Vol. 35(1), pp. 47-61.

Nashif, A.; Jones, D.; Henderson, J. (1985): Vibration damping, Wiley, New York.

Okazaki, A.; Urata, Y.; Tatemichi, A. (1990): Damping properties of three layered shallow spherical shells with a constrained viscoelastic layer. *JSME Int J Series I*, Vol. 33(2), pp. 145-151.

Pahr, D. H.; Rammerstorfer, F. G. (2006): Buckling of honeycomb sandwiches: periodic finite element considerations. *CMES: Computer Modeling in Engineering & Sciences.* Vol. 13, No. 1, pp. 19-34.

Pei, J.; Issam, E. H. (1992): Axisymmetric general shells and jointed shells of revolution. *J. of Structural Engg*, Vol. 118(11), pp. 3186-3202.

Pradeep, V.; Ganesan, N.; Padmanabhan, C. (2006): Buckling and vibration behaviour of a viscoelastic sandwich cylinder under thermal environment. *Int. J. for Computational Methods in Engineering Science and Mechanics,* Vol. 7, pp. 389-401.

Ramasamy, R.; Ganesan, N. (1999): Vibration and damping analysis of fluid filled orthotropic cylindrical shells with constrained viscoelastic damping. *Computers and Struct,* Vol. 70, pp.363-376.

Shiah, Y. C.; Lin, Y. C.; Tan, C. L. (2006): Boundary element stress analysis of thin layered anisotropic bodies. *CMES: Computer Modeling in Engineering & Sciences.* Vol. 16, No. 1, pp.

15-26.

Singh, A. V.; Subramaniam, L. (2003): Vibration of thick circular disks and shells of revolution. *ASME J. of Applied Mechanics*, Vol. 70, pp. 292-298.

Sivadas, K. R.; Ganesan, N. (1992): Vibration analysis of thick composite clamped conical shells of varying thickness. *J. Sound and Vibration*, Vol. 152(1), pp.27-37.

Sivadas, K. R. (1995): Vibration analysis of pre stressed thick circular conical composite shells. *J. Sound and Vibration*, Vol. 186(1), pp. 87-97

Tan, D. Y. (1998): Free vibration analysis of shells of revolution. *J. Sound and Vibration*, Vol. 213(1), pp. 15-33.

Wilkins, D. J.; Bert, C. W.; Egle, D. M. (1970): Free vibration of orthotropic sandwich conical shells with various boundary conditions. *J. of Sound and Vibration*. Vol. 13, pp. 211-28.

Yuh, C. H.; Shyh, C. H. (2000): The frequency response and damping effect of three layer thin shell with viscoelastic core. *Computers and Struct*, Vol. 76, pp. 577-591.